

Deformation relief and grain boundary energy in the zone of local tetragonal-monoclinic transformation in yttria-stabilized zirconia

© T.V. Kozlova, I.N. Sevostyanova, G.V. Shlyakhova, S.P. Buyakova

Institute of Strength Physics and Materials Science, Siberian Branch, Russian Academy of Sciences, Tomsk, Russia
E-mail: kozlovatv@ispms.ru

Received May 22, 2024

Revised August 7, 2024

Accepted August 7, 2024

Atomic force microscopy was used to study the local tetragonal-monoclinic transformation under load in yttria-stabilized zirconia with different grain sizes near the Vickers indentation crack propagation zone. It was shown that an increase of the sintering temperature and holding time leads to a decrease in the grain boundary energy. The local tetragonal-monoclinic transformation and the formation of self-accommodating variant pairs of the martensite type lead to a decrease in the grain boundary energy and stress relaxation.

Keywords: yttria stabilized zirconia (Y-TZP), atomic force microscopy, tetragonal-monoclinic transformation under load, grain boundary energy.

DOI: 10.61011/TPL.2025.01.60127.20000

Tetragonal phase yttria stabilized zirconia (Y-TZP) has a unique mechanism for increasing fracture toughness when the tetragonal phase (t) is transformed into monoclinic (m) in internal stress fields [1–3]. The martensitic transformation of $t \rightarrow m$ in Y-TZP is accompanied by a positive dilatation effect of 3–4% and a shear strain value $\sim 10\%$ [2], while the compressive stresses in the martensitic transformation zone $t \rightarrow m$ prevent crack propagation and lead to strengthening of the ceramics [2,3].

A promising method for studying the martensitic relief on the Y-TZP surface, which arises as a result of the $t \rightarrow m$ transformation, is atomic force microscopy (AFM) [4–7], which allows studying the structure characteristics in a three-dimensional representation with high vertical and lateral resolution.

The ability to undergo martensitic transformation in Y-TZP is directly related to the grain size [8,9]. Earlier in the work [10] the deformation relief along the propagation of a crack initiated by a Vickers pyramid in Y-TZP was investigated using the AFM microscopy. It was shown that the formation of the relief near the crack propagation zone is caused by the $t \rightarrow m$ transformation. Moreover, the average height and width of the deformation relief increase with increasing grain size. The study was carried out on the polished surface of Y-TZP samples, which does not allow distinguishing the transformation features in individual grains. AFM-images analysis of ceramic surface after thermal etching will provide additional information on the grain interior topology and their boundary energy.

The aim of the work is to study the surface topology and grain boundary energy in the $t \rightarrow m$ local transformation zone in ceramics with different grain sizes using the AFM microscopy.

The ceramics $ZrO_2-5.5 \text{ wt.}\% Y_2O_3$ stabilized in the tetragonal modification was used as the object of study. Samples with different grain sizes were obtained by varying

the temperature and holding time during sintering. Sintering at a temperature of 1500°C for 1, 3 and 5 h resulted in the formation of a structure with average grain sizes of 0.55, 0.7 and $0.8 \mu\text{m}$, respectively. Increasing the sintering temperature to 1600°C with holding time 1, 3, 5 h promotes the growth of average grain sizes to 0.9, 1.1 and $1.55 \mu\text{m}$ respectively. Heating and cooling rate was $4^\circ\text{C}/\text{min}$. The density of the samples in different sintering modes calculated hydrostatically was $98 \pm 1\%$ of the theoretical one. To identify the grain boundaries of the ceramics, thermal etching of the polished surface of the samples was carried out in an air furnace at a temperature of 1500°C and a holding time of 25 min. Indentation of polished samples was carried out on a „Super-Vickers“ hardness tester at a load of 100 N with a holding time of 15 s.

The study of the relief near the Vickers indentation angle and the crack propagation zone was carried out using a Solver PRO-47H Atomic Force Microscope. AFM-analysis of the ceramic surface was carried out in two modes: contact mismatch method and semi-contact „phase“ method. The image formation in the Phase Imaging Mode is determined by the total interaction of the elastic force at the contact moment and the Van der Waals forces [11]. While changes in the phase lag reflect local changes in the elastic moduli on the surface of the sample.

The grain boundary energy was calculated from three-dimensional AFM-images ($10 \times 10 \mu\text{m}$) by measuring the dihedral angle of the thermal groove. The measurement technique was first proposed by Mullins [12] and is based on the equilibrium of tensile forces at the grain boundary:

$$\gamma = \frac{\gamma_b}{\gamma_s} = 2 \cos \frac{\psi}{2}, \quad (1)$$

where γ — relative grain boundary energy, γ_b and γ_s — grain boundary and surface energies, respectively, ψ — dihedral angle of the thermal etching groove.

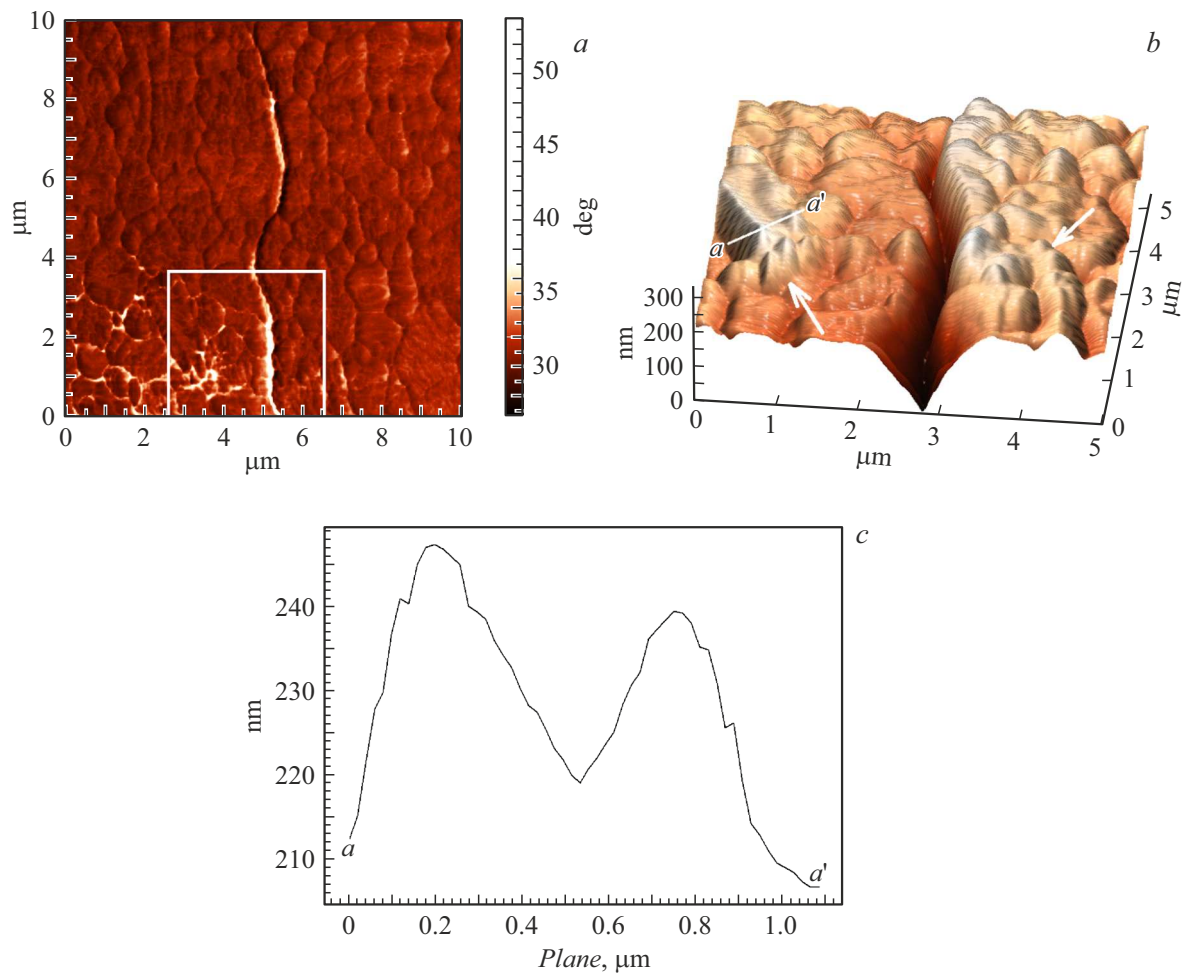


Figure 1. *a* — Phase mode AFM-image of Y-TZP with average grain size $d = 1.55 \mu\text{m}$; *b* — 3D AFM-image of a surface topology marked at a ; *c* — cross-section profile $a-a'$.

Earlier in [10] by the analysis of AFM profiles it was shown that the deformation relief near the angle of the Vickers pyramid imprint and along the crack propagation in $\text{ZrO}_2-5.5 \text{ wt.}\% \text{ Y}_2\text{O}_3$ is formed in all samples despite on the grain size. However, the widest areas of the transformed structure with high deformation relief are observed in samples with a maximum grain size of $d = 1.55 \mu\text{m}$. Therefore, for the detailed AFM-study of the characteristics of the $t \rightarrow m$ transformation in ceramics under load a sample with the maximum grain size was selected.

Fig. 1 shows AFM-images of the Y-TZP structure with an average grain size of $1.55 \mu\text{m}$ close to the indentation and the crack propagation zone. The indentation zone is located at the bottom of the image. At phase mode images (Fig. 1, *a*) light areas are visible close to the imprint, along the crack, at grain boundaries and at triple junctions. Ceramic samples with $d = 0.55-1.10 \mu\text{m}$ are characterized by narrower areas of altered phase contrast than samples with $d = 1.55 \mu\text{m}$.

For a detailed analysis of the ceramic surface topology, the region highlighted by the light frame in Fig. 1, *a* is presented as a three-dimensional AFM-image in Fig. 1, *b*.

It is evident that along the crack propagation path and in individual favorably oriented grains near it, an N -shaped deformation relief is formed, characteristic of a diffusion-free martensitic transformation. The $a-a'$ profile of the transformed grain is shown in Fig. 1, *c*. Similar structures were observed in [1] cesium-stabilized zirconium dioxide. The authors showed that high stresses formed at the crack tip promote the $t \rightarrow m$ transformation, and this primarily occurs for favorably oriented grains with crystallographic axis c perpendicular to the scanned surface. While the crack is stationary, stresses increase in its vicinity. As soon as these stresses become high enough the $t \rightarrow m$ transformation starts in these zones, decompresses part of the stresses [1].

The 3D image (Fig. 1, *b*) shows that at triple junctions and at grain boundaries in the zone of altered phase contrast, a deformation relief typical for invariant plane deformation is formed in the form of self-accommodating variant pairs of surface elevations associated with the dilatation effect (marked with arrows). According to [13], the formation of self-accommodating variant pairs is directly related to the micro- and macroscopic effects of local shifts and stresses

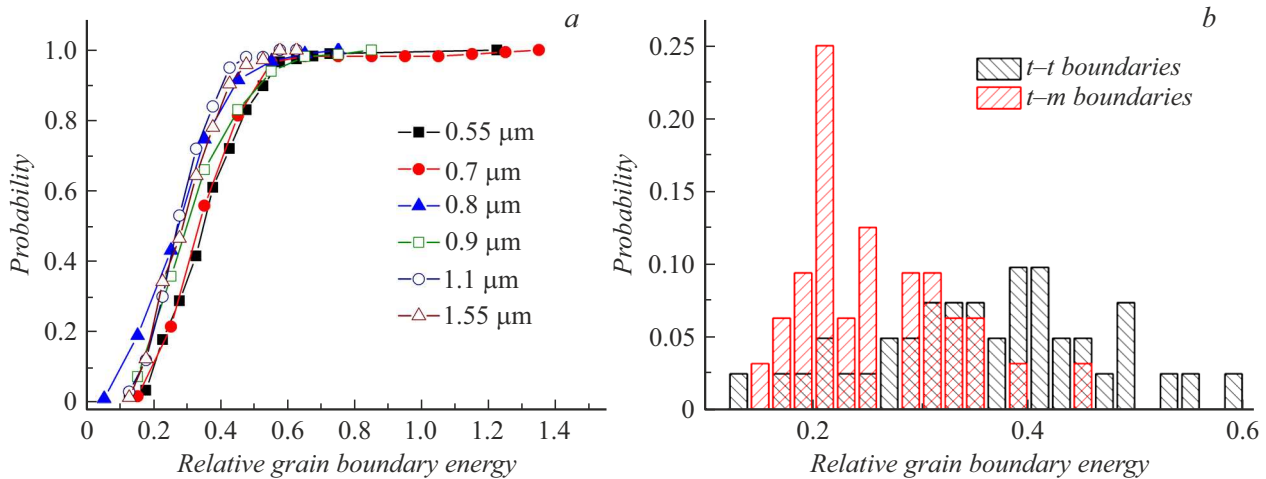


Figure 2. *a* — relative grain boundary energy in Y-TZP ceramics after sintering under different conditions; *b* — energy distribution of interphase $t-m$ and intraphase $t-t$ boundaries.

arising as a result of the $t \rightarrow m$ transformation. Residual stresses arising from mechanical action on the material are concentrated in grain boundaries and triple junctions, which act as preferred centers for the martensite formation.

Fig. 2, *a* shows the cumulative distribution functions (CDF) of the boundary energy in ceramics with different grain sizes. It can be seen that the proportion of low-energy boundaries ($\gamma < 0.5$) for all states is more than 80%. Differences between data sets characteristic of different sintering conditions are observed only in the high-energy region. The CDFs of grain boundary energies for samples with average grain sizes $\langle d \rangle = 0.55$ and $0.7 \mu\text{m}$ shift towards higher values. This indicates that high-energy boundaries ($\gamma = 1-1.5$) remain in the ceramic structure after sintering at a lower temperature. An increase in the sintering temperature and holding time leads to a narrowing of the energy range at the CDFs to $\gamma = 0.08-1.0$. This is mainly due to the decrease in the entropic contribution to free energy with increasing temperature. The observed grain growth with increasing temperature and holding time of ceramic samples leads to a decrease in the total interphase surface area mainly due to the annihilation of high-energy boundaries. An additional factor in the decrease in grain boundary energy with increasing sintering temperature may be an increase in the concentration of yttrium in the grain boundary regions, as shown in work [14].

The contribution of the $t \rightarrow m$ interphase boundaries to the energy distribution should be considered separately. The interphase boundaries are most clearly revealed in AFM-images of ceramics with grain sizes $d = 1.55 \mu\text{m}$. Local grain boundary energy estimation were carried out near the indentation and in the crack propagation zone in areas with deformation relief along the crack (Fig. 1, *b*) and areas corresponding to light zones in the phase mode, which presumably belong to monoclinic grains (Fig. 1, *a*). The obtained estimates were compared with the energy distribution for intraphase $t-t$ grain boundaries located far

from the crack. It is evident (Fig. 2, *b*) that the differential energy distribution function of the interphase boundaries $t-m$ lies in the low-energy region ($\gamma = 0.1-0.4$), and the average energy value of the interphase boundaries $t-m$ is 2 times lower. This indicates the stress relaxation at grain boundaries due to the local $t \rightarrow m$ transformation and the formation of self-accommodating variant pairs at grain boundaries and in triple junctions, i.e., the change in grain boundary energy may indirectly indicate the $t \rightarrow m$ transformation that has taken place in the ceramic structure.

Thus, the analysis of 3D-images of the surface of Y-TZP samples after thermal etching made it possible to identify the deformation relief in individual grains near the Vickers pyramid imprint and along the crack propagation, as well as to study its local characteristics. It was determined that in the areas along the crack and in individual favorably oriented grains near it, the $t \rightarrow m$ transformation occurs. It is shown that the formation of martensitic structures is observed in areas of maximum stress, namely at grain boundaries and in triple junctions. It was established that a decrease in the grain boundary energy can serve as an indicator of the $t \rightarrow m$ transformation that has taken place in the ceramic structure.

The work has been performed under the state assignment of ISPMS SB RAS (project No. (FWRW-2021-0009 and FWRW-2021-0011).

Conflict of interest

The authors declare that they have no conflict of interest.

References

- [1] J. Chevalier, L. Gremillard, A.V. Virkar, D.R. Clarke, J. Am. Chem. Soc., **92** (9), 1901 (2009). DOI: 10.1111/j.1551-2916.2009.03278.x
- [2] M. Trunec, Ceram. Silik., **52** (3), 165 (2008). https://www.ceramics-silikaty.cz/2008/pdf/2008_03_165.pdf

- [3] R.H.J. Hannink, P.M. Kelly, B.C. Muddle, *J. Am. Ceram. Soc.*, **83** (3), 461 (2000). DOI: 10.1111/j.1151-2916.2000.tb01221.x
- [4] S. Deville, G. Guénin, J. Chevalier, *Acta Mater.*, **52** (19), 5709 (2004). DOI: 10.1016/j.actamat.2004.08.036
- [5] M. Mamivand, M.A. Zaeem, H. El Kadiri, *Acta Mater.*, **87**, 45 (2015). DOI: 10.1016/j.actamat.2014.12.036
- [6] H. Tsubakino, Y. Kuroda, M. Niibe, *J. Am. Ceram. Soc.*, **82** (10), 2921 (1999). DOI: 10.1111/j.1151-2916.1999.tb02180.x
- [7] X.Y. Chen, X.H. Zheng, H.S. Fang, H.Z. Shi, X.F. Wang, H.M. Chen, *J. Mater. Sci. Lett.*, **21**, 415 (2002).
- [8] M. Trunec, Z. Chlup, *Scripta Mater.*, **61** (1), 56 (2009). DOI: 10.1016/j.scriptamat.2009.03.019
- [9] I.R. Crystal, Ch.A. Schuh, *Acta Mater.*, **209**, 116789 (2021). DOI: 10.1016/j.actamat.2021.116789
- [10] T.Y. Sablina, I.N. Sevostyanova, G.V. Shlyakhova, *Russ. Phys. J.*, **65** (4), 635 (2022). DOI: 10.1007/s11182-022-02679.
- [11] <https://www.parksystems.com>
- [12] W.W. Mullins, *Acta Met.*, **6** (6), 414 (1958). DOI: 10.1016/0001-6160(58)90020-8
- [13] S. Deville, H. El Attaoui, J. Chevalier, *J. Eur. Ceram. Soc.*, **25** (13), 3089 (2005). DOI: 10.1016/j.jeurceramsoc.2004.07.029
- [14] K. Matsui, N. Ohmichi, M. Ohgai, H. Yoshida, Y. Ikuhara, *J. Ceram. Soc. Jpn.*, **114** (1327), 230 (2006). DOI: 10.2109/jcersj.114.230

Translated by D.Safin